Dielectric surface and capping effects on optical properties of a few atomic monolayer thick MoS_2

D. Sercombe,[*,†] S. Schwarz,[†] O. Del Pozo-Zamudio,[†] F. Liu,[‡] B. J. Robinson,[¶] E. A. Chekhovich,[†] I. I. Tartakovskii,[§] O. Kolosov,[¶] and A. I. Tartakovskii[*,†]

Department of Physics and Astronomy, University of Sheffield, Sheffield S3 7RH, UK, Technische Universitat Dortmund, Dortmund, Department of Physics and Astronomy, University of Lancaster, and Institute of Solid State Physics, Russian Academy of Sciences, Chernogolovka, 142432, Russia

E-mail: php10ds@sheffield.ac.uk; a.tartakovskii@sheffield.ac.uk

Abstract

We use micro-photoluminescence (PL) and ultrasonic force microscopy to explore the effects of dielectric substrate and capping on optical properties of a few mono-layer MoS_2 films. PL lineshapes and peak energies for uncapped films are found to vary widely. This non-uniformity is dramatically suppressed by capping with SiO_2 and Si_xN_y, improving mechanical coupling of MoS_2 with the surrounding dielectrics. Capping also leads to pronounced charging of the films, evidenced from the dominating negative trion peak in PL.

[*]To whom correspondence should be addressed
[†]University of Sheffield
[‡]Technische Universitat Dortmund
[¶]University of Lancaster
[§]Institute of Solid State Physics

Introduction

Interest in atomically thin two-dimensional (2D) layered compounds is growing due to unique physical properties found for monolayer (ML) structures.[1,2] One such material, molybdenum disulfide (MoS_2), has generated particular interest due to the presence of an indirect-to-direct band gap transition and observation of photoluminescence (PL)[3–5] and electro-luminescence[6] in the visible range up to room temperature. A high on/off ratio (exceeding 10^8) has suggested a potential use in field effect transistors,[7] while a strong valley polarization is likely to be used in the development of future valleytronics applications.[8–12]

PL studies[4] have shown that suspended ML films of MoS_2 have an enhanced emission compared to those in contact with the substrate, demonstrating a strong effect of surface interactions on optical properties of MoS_2 films. The eventual integration of MoS_2 into devices, such as transistors and photonic structures, will render the use of suspended MoS_2 impractical. The effect of capping has so far been reported for high-*k* dielectric materials commonly used in transistors.[13–15] However, no detailed study showing how dielectric environments affect MoS_2 PL properties has yet been conducted, an issue we address within this work.

Here we focus on interaction of MoS_2 films with SiO_2 and Si_xN_y commonly used in photonic devices, and report low temperature PL measurements on over a 100 thin films, enabling detailed insight in interaction of MoS_2 with its dielectric surrounding. We study mechanically exfoliated MoS_2 films deposited on silicon substrates finished with either nearly atomically flat thermally grown SiO_2 or relatively rough SiO_2 grown by plasma-enhanced chemical vapor deposition (PECVD). For this we use a combination of low temperature micro-photoluminescence (PL), atomic force microscopy (AFM) and ultrasonic force microscopy (UFM). We find marked variety of the PL spectral lineshapes and peak energies in the large number of few monolayer MoS_2 films, which nonetheless show trends that we are able to relate to electrostatic and mechanical interaction of thin films with the surrounding dielectrics.

We find, that films without additional dielectric capping (referred to below as 'uncapped') on both types of substrates show marked variation of the PL peak positions, E_{max} and variations in the

PL linewidths, ΔE_{FWHM}. Such non-uniformities are particularly pronounced in uncapped MoS_2 films on rough PECVD substrates. By coating samples with SiO_2 and Si_xN_y, we observe markedly narrowed distributions of E_{max} and ΔE_{FWHM}, leading to significantly more reproducible PL characteristics. We also find that capping with either SiO_2 or Si_xN_y leads to relative enhancement of a negatively charged trion PL peak, particularly prominent in MoS_2 films on flat thermal oxide substrates.

In order to explore this behavior further we used the ability of UFM to probe the stiffness of the thin films below the capping layer. We demonstrate that variations in spectral properties are related to how the roughness of the underlying substrate affects the MoS_2 morphology and mechanical coupling between the MoS_2 film and the surrounding layers. We find that high mechanical coupling between the film and the surrounding layers is only possible for capped films on thermally grown SiO_2, whereas more complex morphology and poorer contact with the surrounding layers is observed for uncapped films, the effect further exacerbated for films on PECVD substrates. We thus argue that the variations in the PL lineshape and peak position originate from inhomogeneity in charging and (possibly) strain, suppressed for MoS_2 films on flat thermally grown SiO_2 substrates, and further improved by capping with dielectrics, showing this as a viable method for creating uniform optical properties in photonic devices comprising 2D films.

Experimental procedure

Sample preparation. MoS_2 was exfoliated using the mechanical cleavage method[1] and deposited on commercially purchased Si wafers with a low roughness 300 nm thick thermally grown SiO_2.[16] Further MoS_2 samples were produced using the same technique, but deposited on Si substrates covered with 300 nm PECVD grown SiO_2. PECVD deposition was done in a 60^oC chamber with a sample temperature of 300^oC. The root mean square (rms) roughness, R_{rms}, of the PECVD grown SiO_2 is found to be 2 nm with a maximum peak height of 15 nm, whereas R_{rms} of the thermally grown SiO_2 is 0.09 nm with a maximum height of 0.68 nm. The thin MoS_2 films had optical contrasts corresponding to thicknesses of 2-5 MLs, confirmed by AFM on thermal oxide substrates. Capping of the films with Si_xN_y and SiO_2 was done using the same PECVD techniques with layer thicknesses of 100 nm for PL and 15 nm for AFM/UFM measurements.

Micro-photoluminescence experiments. Low temperature (10K) micro-PL was carried out on a large number of thin films in a continuous flow He cryostat. The signal was collected and analyzed using a single spectrometer and a nitrogen-cooled charged-coupled device. The sample was excited with a laser at 532 nm. All PL spectra presented in this work were measured in a range of low powers where no dependence on power of PL lineshape was found.

AFM/UFM experiments. As shown elsewhere,[17] the ultrasonic force microscopy (UFM) allows imaging of the near-surface features and subsurface interfaces with superior nanometre scale resolution of AFM techniques.[18] In the sample-UFM modality used in this paper,[19] the sample in contact with the AFM tip is vibrated at small amplitude (0.5-2 nm) and high frequency (2-10 MHz), much higher than the resonance frequencies of the AFM cantilever. The resulting sample stress produces reaction force, that is modified by the voids, subsurface defects or sample-substrate interfaces, and can be detected as an additional 'ultrasonic' force. A unique feature of UFM is that it enables nanometre scale resolution imaging of morphology of subsurface nano-structures and interfaces of solid-state objects. In order to interpret the images of a few layer films presented in Fig.5, one can note that the bright (dark) colors correspond to higher (lower) sample stiffness.

Results

PL of thin MoS_2 films

Fig. 1(a) shows a selection of PL spectra measured for a few ML uncapped MoS_2 films deposited on Si substrates with either PECVD (a-d) or thermal oxidation (e-h). In all spectra exciton complexes A and B are clearly visible,[3] though there is a large variation in PL lineshapes for different films. The A complex is composed of a trion PL peak A^- and a high energy shoulder A^0 corresponding to neutral exciton PL.[20] A low energy shoulder L is also observed in some spectra, though

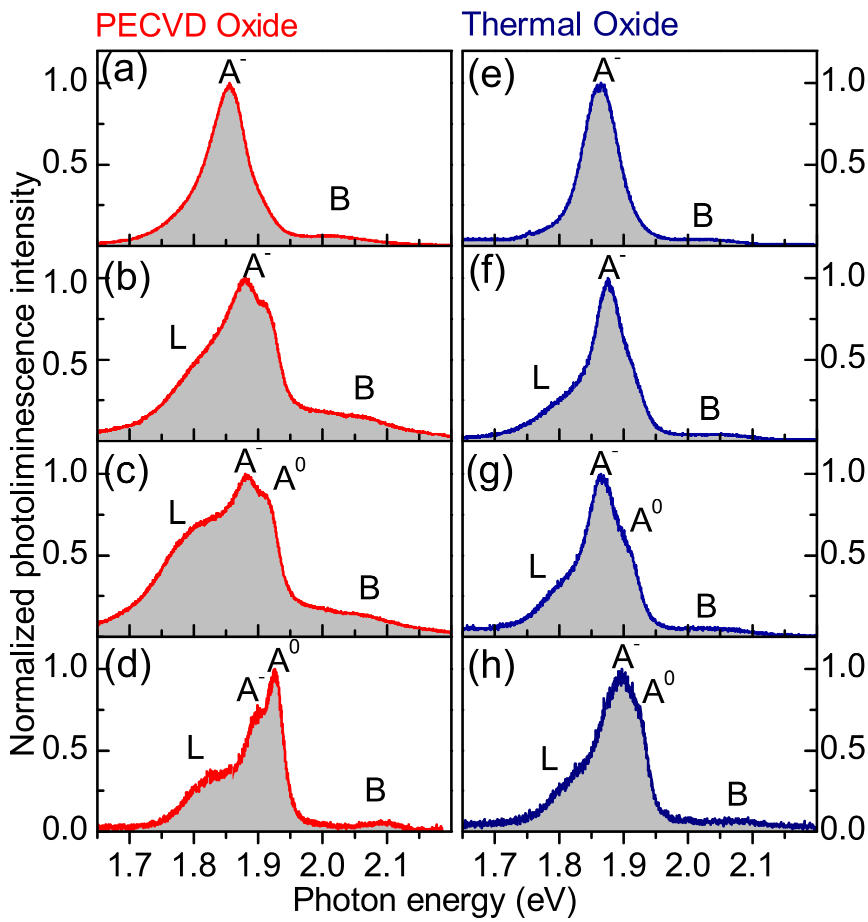

Figure 1: PL spectra measured for individual mechanically exfoliated MoS_2 uncapped films deposited on a 300 nm SiO_2 layer grown by either PECVD (a-d) or thermal oxidation (e-h) on a silicon substrate.

spectra showing weak or no contributions of L and A^0 states were observed on both PECVD (a) and thermal oxide (e) substrates. A relatively large contribution of L and A^0 was found in many films deposited on PECVD substrates (b, c) and in some cases the neutral exciton was found to have brighter emission than the trion [as in (d)]. For films deposited on thermal oxide substrates, there is a less significant variation in the lineshape (e-h), and L and A^0 features are, in general, less pronounced relative to A^- than in films deposited on PECVD grown SiO_2.

The effect of capping of MoS_2 films with dielectrics is demonstrated in Fig.2. A 100 nm thick film of either SiO_2 or Si_xN_y is deposited using PECVD on films deposited on both PECVD and thermal SiO_2 substrates. Here we observe even less variation in lineshapes between the films. A

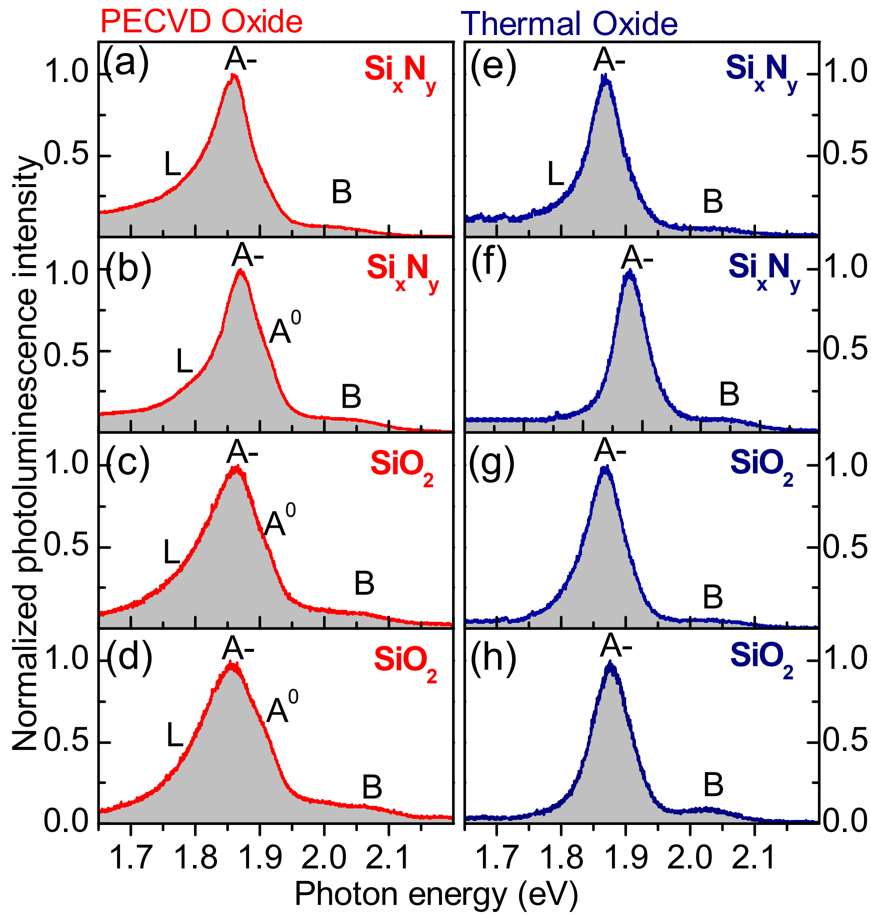

Figure 2: PL spectra measured for individual mechanically exfoliated MoS_2 films capped by a 100 nm PECVD layer of dielectric material. The effect of capping is shown for films deposited on PECVD grown SiO_2 substrates for SiN (a, b) and SiO_2 (c, d) capping layers, and also for films deposited on thermally grown SiO_2 and capped with SiN (e, f) and SiO_2 (g, h).

further suppression of the low energy shoulder L and neutral exciton peak A^0 is found for films capped with Si_xN_y (a,b,e,f) on both types of substrates, and with SiO_2 on thermally grown substrates. In contrast, L and A^0 peaks are pronounced when capping with SiO_2 is used for MoS_2 films on PECVD substrates. Further to this, from comparison of spectra in (a,b,c,d) and (e,f,g,h), we find that the PL linewidths of films deposited on the PECVD oxide are notably broader than for those on the thermal oxide substrates.

An interesting trend in all spectra presented in Figs.1 and 2 is a correlation between the intensities of the features L and A^0: the two peaks are either both rather pronounced or suppressed in any given spectrum relative to the trion peak A^-. This may imply that peak L becomes suppressed

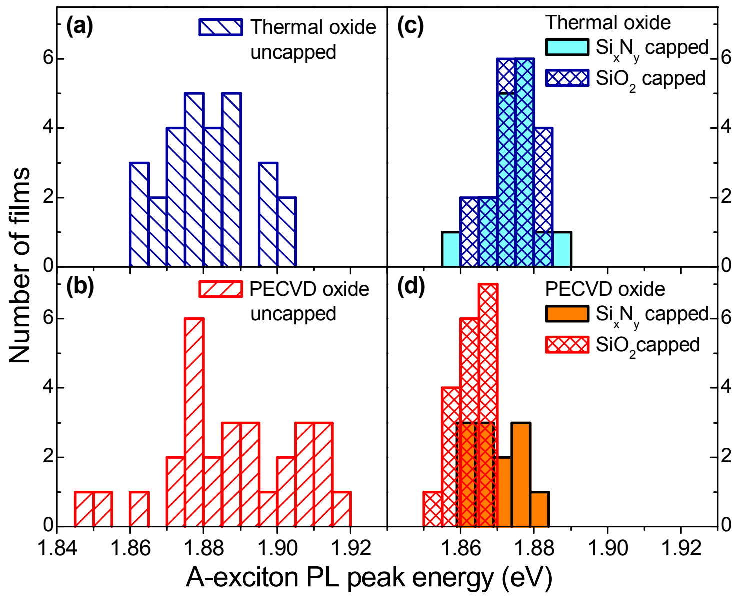

Figure 3: (a-d) PL peak energies for *A* exciton complex in MoS_2 thin films. Data for films deposited on thermally (PECVD) grown SiO_2 substrates are shown in top (bottom) panels. Panels (a)-(b) and (c)-(d) show PL peak positions for uncapped and capped films, respectively.

when the film captures an excess of negative charge.

Analysis of PL peak energies

A statistical analysis of PL peak energies for films deposited on the two types of substrates is presented in Fig.3. Fig.3a,b show that the average values for the PL peak energies, E_{max}^{av}, for uncapped films are $E_{max}^{av} = 1.888$ eV for the PECVD substrates and $E_{max}^{av} = 1.88$ eV for thermal oxide substrates, with an almost two times larger standard deviation, σ_{Emax} for the former (18 versus 11 meV). The data collected for the capped films (shaded for Si_xN_y and hatched for SiO_2) are presented in Fig.3(c) and (d) for the thermal and PECVD oxide substrates, respectively. Significant narrowing of the peak energy distribution is found in all cases: $\sigma_{Emax} \approx$6 meV has been found. The average peak energies are very similar for both SiO_2 and Si_xN_y capping on the thermal oxide substrates (E_{max}^{av}=1.874 eV), but differ for PECVD substrates: E_{max}^{av}=1.862 and 1.870 eV for SiO_2 and Si_xN_y capping, respectively.

From previous reports,[4] for films with thicknesses in the range 2 to 5 MLs, one can expect the PL peak shift on the order of 20 meV. In addition, PL yield was reported to be about 10 times higher for 2 ML films compared with 4 ML and for 3 ML compared with 5 ML.[4] In our study, the integrated PL signal shows a large variation within about one order of magnitude between the films. The dependence of the PL yield on the type of the substrate and capping is not very pronounced. While our data for PL intensities is consistent with the reported in the literature for the range of thicknesses which we studied, the PL peak energy distribution shows the unexpected broadening for uncapped samples: for example, deviations from E^{av}_{max} by $\pm$20-30 meV are evident in Fig.3. For the capped samples, new trends are observed: the significant narrowing and red-shift of E_{max} distributions. As shown below, these effects reflect changes in the PL lineshapes between the capped and uncapped samples, which in their turn reflect changes in the relative intensities of the A^-, A^0 and L peaks.

Analysis of PL lineshapes

In this section we will present the lineshape analysis for the A exciton PL based on the measurement of full width at half maximum (FWHM) in each PL spectrum. This approach allows to account for contributions of the three PL features, L, A^0 and A^-. The data are summarized in Fig.4 and Tables 1.

PECVD grown SiO_2 substrates. These data are presented in Fig.4 in red. Data for uncapped films are shown in Fig.4(a), from where it is evident that the lineshapes vary dramatically from film to film within a range from 50 to 170 meV. FWHM for uncapped films on PECVD grown substrates is on average ΔE^{av}_{FWHM}=96 with a large standard deviation σ_{FWHM}=33 meV. This gives a rather high coefficient of variation $\sigma_{FWHM}/\Delta E^{av}_{FWHM}$=0.34 showing normalized dispersion of the distribution of the PL FWHM.

The non-uniformity of lineshapes of the PL spectra is significantly suppressed by capping the films with Si_xN_y and SiO_2 (shown with red in Fig.4(b) and (c), respectively). This is evidenced from the reduction of the coefficient of variation in the FWHM values by a factor of 4 in capped films compared with the uncapped samples (in Table 1). Despite the narrowed spread of ΔE_{FWHM}

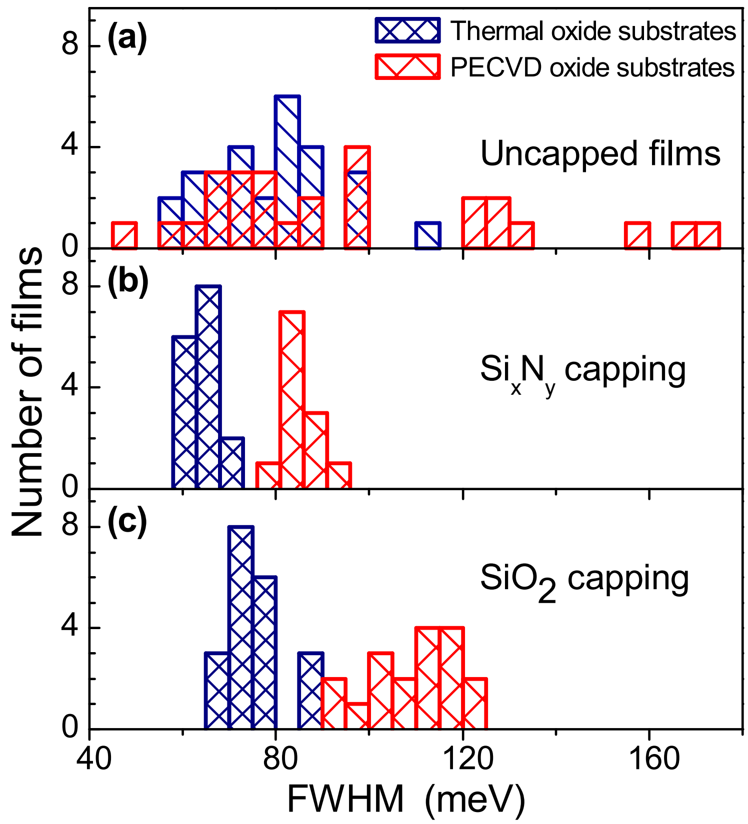

Figure 4: PL FWHM of exciton complex A in thin MoS_2 films. Data for MoS_2 films deposited on thermally and PECVD grown SiO_2 substrates is shown with blue and red, respectively. (a) PL FWHM of uncapped MoS_2 films. (b) PL FWHM of Si_xN_y capped MoS_2 films. (c) PL FWHM of SiO_2 capped MoS_2 films.

values, the average FWHM in SiO_2 capped films is rather high, 109 meV, which reflects relatively strong contribution of L and A^0 PL features. Contributions of A^-, L and A^0 features vary very considerably in the uncapped samples, leading to on average smaller linewidths but a very considerable spread in FWHM values. In contrast, in Si_xN_y capped films, A^- peak dominates and both L and A^0 features are relatively weak, which effectively results in narrowing of PL.

Thermally grown SiO_2 substrates. These data are presented in Fig.4 in blue. It can be seen that uncapped films deposited on the flatter thermal oxide substrates appear to have significantly narrower distributions of linewidths compared to uncapped films on PECVD substrates: coefficient of variation of ΔE_{FWHM} is by a factor of 2 smaller for films on the thermally grown substrates [see Fig.4(a) and Table 1]. In addition, compared with the films deposited on PECVD grown SiO_2,

Table 1: Mean values, standard deviations and coefficients of variation for full width at half maximum of PL spectra measured for thin MoS_2 films.

Substrate/Capping	Mean value	Standard deviation	Coefficient of variation
PECVD/uncapped	96 meV	33 meV	0.34
PECVD/SiO_2	109 meV	9 meV	0.08
PECVD/Si_xN_y	84 meV	7 meV	0.08
Thermal/uncapped	79 meV	12 meV	0.15
Thermal/SiO_2	76 meV	7 meV	0.09
Thermal/Si_xN_y	64 meV	4 meV	0.06

FWHM is also reduced by about 20% to 79 meV. Such narrowing reflects weaker contribution of L and A^0 peaks in PL spectra.

The non-uniformity of the PL spectra still present in uncapped films deposited on thermally grown SiO_2 is further suppressed by capping the films with Si_xN_y and SiO_2 [shown with blue in Fig.4(b) and (c), respectively]. In general, the coefficients of variation for FWHM of the capped films are rather similar for both substrates and are in the range of 0.06-0.09, showing significant improvement of the reproducibility of PL features compared with the uncapped samples (see Table 1). For Si_xN_y capped films on thermally grown SiO_2, we also observe narrowing of PL emission to ΔE^{av}_{FWHM}=64 meV. This reflects further suppression of L and A^0 peaks relative to A^-, the effect less pronounced in SiO_2 capped films.

AFM and UFM measurements

To further understand the interactions between MoS_2 films and the substrate/capping materials, we carried out detailed AFM and UFM measurements of our samples (Fig.5). AFM measurements of films deposited on PECVD grown substrates Fig.5(a) show that the film is distorted in shape and follows the morphology of the underlying substrate. The R_{rms} of these films is 1.7 nm with a maximum height R_{max}=11 nm, similar to the parameters of the substrate, R_{rms}=2 nm and R_{max}=15 nm. Such R_{max} is greater than the thickness of films (<3 nm), leading to significant film distortions.

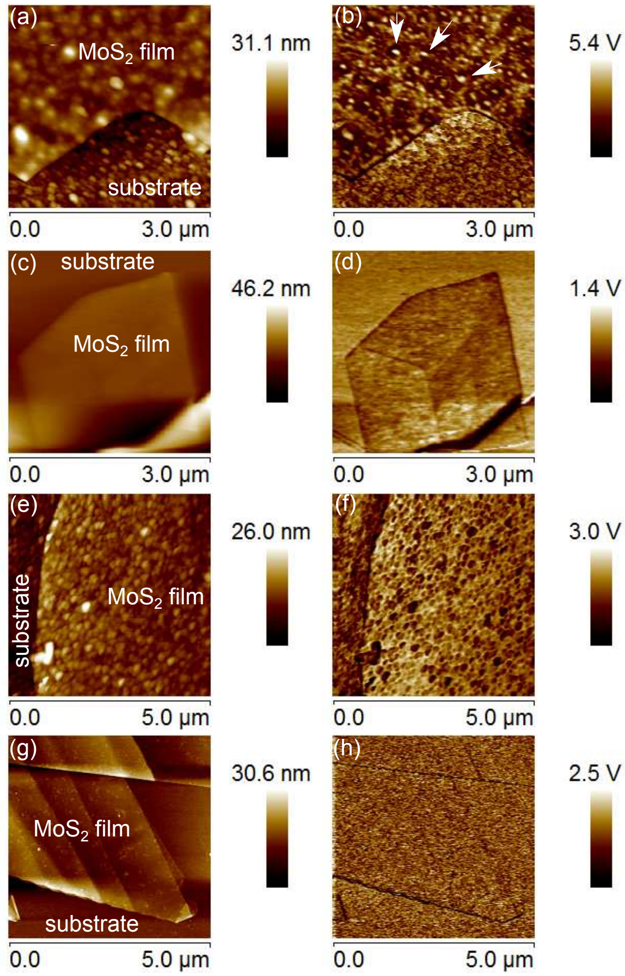

Figure 5: AFM (left column) and UFM (right column) images for MoS_2 thin films deposited on PECVD and thermally grown SiO2 substrates. (a,b) PECVD substrate, uncapped MoS_2 film; (c,d) thermally grown substrate, uncapped MoS_2 film; (e,f) PECVD substrate, MoS_2 film capped with 15 nm of SiO_2 grown by PECVD; (g,h) thermally grown substrate, MoS_2 film capped with 15 nm of SiO_2 grown by PECVD.

UFM measurements of these films [Fig.5(b)] show small areas of higher stiffness (light colour, marked with arrows) and much larger areas of low stiffness (i.e. no contact with the substrate) shown with a dark colour. This shows that the film is largely suspended above the substrate on point contacts.

AFM measurements of films deposited on thermally grown SiO_2 substrates [Fig.5(c)] show a much more uniform film surface due to the less rough underlying substrate. This is reflected in a significantly improved R_{rms} = 0.3 nm and R_{max}=1.8 nm. These values are still higher than those for the bare substrate with R_{rms} = 0.09 nm and R_{max}=0.68 nm. A more uniform stiffness distribution is observed for these films in UFM [Fig.5(d)], though the darker colour of the film demonstrates that it is much softer than the surrounding substrate and thus still has relatively poor contact with the substrate. A darker shading at film edges demonstrates that they have poorer contact than the film centre and effectively curl away from the substrate.

AFM and UFM data for films capped with 15 nm SiO_2 after deposition on PECVD and thermally grown SiO_2 are given in Fig.5(e, f) and (g, h), respectively. For the PECVD substrate, the roughness of the MoS_2 film is similar to that in the uncapped sample in Fig.5(a): R_{rms}=1.68 nm and R_{max}=10.2 nm. From the UFM data in Fig.5(f), it is evident that although the contact of the MoS_2 film with the surrounding SiO_2 is greatly improved compared with the uncapped films, a large degree of non-uniformity is still present, as concluded from many dark spots on the UFM image. In great contrast to that, the capped MoS_2 film on thermally grown SiO_2 is flatter [Fig.5(g, h)], R_{rms}=0.42 nm and R_{max}=6.1 nm, with the roughness most likely originating from the PECVD grown SiO_2 capping layer. The UFM image in Fig.5(h) shows remarkable uniformity of the stiffness of the film similar to that of the capped substrate, demonstrating uniform and firm contact (i.e. improved mechanical coupling) between the MoS_2 film and the surrounding dielectrics.

Discussion

There is a marked correlation between the PL properties of the MoS_2 films and film stiffness measured by UFM. The stiffness reflects the strength of the mechanical coupling between the adjacent monolayers of the MoS_2 film and the surrounding dielectrics. The increased bonding and its uniformity for films deposited on less rough thermally grown SiO_2 substrates and for capped MoS_2 films manifests in the more reproducible PL characteristics, leading to reduced standard deviations of the peak positions and linewidths. These spectral characteristics are influenced by the relative intensities of the three dominating PL features, trion A^-, neutral exciton A^0 and low energy L peak, which are influenced by the charge balance in the MoS_2 films sensitive to the dielectric environment. The efficiency of charging can be qualitatively estimated from the relative intensities of A^- and A^0 peaks. In the vast majority of the films, A^- dominates. As noted above, the intensity of A^0 directly correlates (qualitatively) with that of the relatively broad low energy PL shoulder L (see Fig.1 and 2), previously ascribed to emission from surface states. The lineshape analysis presented in Fig.4 and Table 1 is particularly sensitive to the contribution of peak L.

The PL lineshape analysis and comparison with the UFM data lead to conclusion that negative charging of the MoS_2 films is relatively inefficient for partly suspended uncapped films on rough PECVD substrates. Both in SiO_2 and Si_xN_y capped films on PECVD substrates, the charging effects are more pronounced, particularly for Si_xN_y capping. However, both A^0 and L features still have rather high intensities. The relatively low charging efficiency is most likely related to a non-uniform bonding between the MoS_2 films and the surrounding dielectric layers as concluded from from UFM data [see Fig.5(f)]. The charging is more pronounced for uncapped MoS_2 films on thermal oxide substrates, and is enhanced significantly more for capped films: for Si_xN_y capping A^0 and L peaks only appear as weak shoulders in PL spectra.

It is clear from this analysis that the charge balance in the MoS_2 films is altered strongly when the films are brought in close and uniform contact with the surrounding dielectrics, enabling efficient transfer of charge in a monolithic hybrid heterostructure. Both n-type[4,7,21] and p-type[21,22] conductivities have been reported in thin MoS_2 films deposited on SiO_2. It is thus possible that the sign and density of charges in exfoliated MoS_2 films may be strongly affected by the properties of PECVD grown SiO_2 and Si_xN_y, where the electronic properties may vary depending on the growth conditions.[23–25] It is notable, however, that for a large variety of samples studied in this work, the negative charge accumulation in the MoS_2 films is pronounced, and is further enhanced when the bonding of the films with the dielectric layers is enhanced.

The band-structure of MoS_2 and hence its optical characteristics can also be influenced by strain.[26] However, the distribution and magnitude of strain cannot be assessed directly in our experiments. Indirect evidence for strain reduction in capped samples compared to uncapped films on PECVD may be deduced from the red-shift of the average PL peak energy by up to 30 meV after capping (data in Fig.3). One would expect a more uniform strain distribution in the case of uniform mechanical properties of the sample, which as shown by UFM is achieved for capped MoS_2 films on flat thermally grown SiO_2 substrates. Further evidence for increased uniformity of mechanical properties of thin MoS_2 films on flatter thermal oxide substrates is also obtained in our studies of Raman scattering (to be presented elsewhere), where we observed suppressed variation of the frequency of $E^1_{2g}(R)$ vibration mode.[27]

Conclusions

We demonstrate that it is possible to increase the reproducibility of PL properties for mechanically exfoliated few mono-layer MoS_2 films by coating the films with additional dielectric layers of either SiO_2 or Si_xN_y. By comparing PL data with results obtained in UFM, we show that there is a direct correlation between the degree of the mechanical coupling of the MoS_2 films to the surrounding dielectrics and uniformity of the optical properties. We show that a wide spread in PL spectral lineshapes occurs in general as a result of the film-to-film variation of the relative intensities of the negatively charged trion peak A^- and the two other features, neutral exciton peak A^0 and a low energy PL band L. We find that when the mechanical coupling between the films and the dielectrics is improved, the films become increasingly negatively charged, as deduced from the pronounced increase in PL of the trion peak, dominating in the majority of PL spectra. Such charging, and also possibly reduction in strain non-uniformities, underpins the highly uniform PL properties in capped MoS_2 films, leading to the smallest linewidths of around 64 meV for thin MoS_2 films deposited on thermally grown SiO_2 and capped with a Si_xN_y layer.

References

Acknowledgement

This work has been supported by the Marie Curie ITNs S^{3}NANO and Spin-Optronics, and EU FP7 GRENADA grant. O. D. P.-Z. thanks CONACYT-Mexico Doctoral Scholarship.

References

(1) Novoselov, K. S.; Jiang, D.; Schedin, F.; Booth, T. J.; Khotkevich, V. V.; Morozov, S. V.; Geim, A. K. *PNAS* **2005**, *102*, 10451–10453.

(2) Wang, Q. H.; Kalantar-Zadeh, K.; Kis, A.; Coleman, J. N.; Strano, M. S. *Nature Nanotechnology* **2012**, *7*, 699–712.

(3) Splendiani, A.; Sun, L.; Zhang, Y.; Li, T.; Kim, J.; Chim, C.-Y.; Galli, G.; Wang, F. *Nano Letters* **2010**, *10*, 1271–1275.

(4) Mak, K.; Lee, C.; Hone, J.; Shan, J.; Heinz, T. *Phys. Rev. Lett.* **2010**, *105*, 2–5.

(5) Eda, G.; Yamaguchi, H.; Voiry, D.; Fujita, T.; Chen, M.; Chhowalla, M. *Nano Letters* **2011**, *11*, 5111–6.

(6) Sundaram, R. S.; Engel, M.; Lombardo, A.; Krupke, R.; Ferrari, A. C.; Avouris, P.; Steiner, M. *Nano Letters* **2013**, *13*, 1416–1421.

(7) Radisavljevic, B.; Radenovic, a.; Brivio, J.; Giacometti, V.; Kis, a. *Nature Nanotechnology* **2011**, *6*, 147–50.

(8) Mak, K. F.; He, K.; Shan, J.; Heinz, T. F. *Nature Nanotechnology* **2012**, *7*, 494–8.

(9) Sallen, G.; Bouet, L.; Marie, X.; Wang, G.; Zhu, C.; Han, W.; Lu, Y.; Tan, P.; Amand, T.; Liu, B.; Urbaszek, B. *Phys. Rev. B* **2012**, *86*, 3–6.

(10) Zeng, H.; Dai, J.; Yao, W.; Xiao, D.; Cui, X. *Nature nanotechnology* **2012**, *7*, 490–3.

(11) Cao, T.; Wang, G.; Han, W.; Ye, H.; Zhu, C.; Shi, J.; Niu, Q.; Tan, P.; Wang, E.; Liu, B.; Feng, J. *Nature Communications* **2012**, *3*, 887.

(12) Xiao, D.; Liu, G.-B.; Feng, W.; Xu, X.; Yao, W. *Phys. Rev. Lett.* **2012**, *108*, 196802.

(13) Jena, D.; Konar, A. *Phys. Rev. Lett.* **2007**, *98*, 136805.

(14) Plechinger, G.; Schrettenbrunner, F.-X.; Eroms, J.; Weiss, D.; Schüller, C.; Korn, T. *Phys. Status Solidi RRL* **2012**, *6*.

(15) Yan, R.; Bertolazzi, S.; Brivio, J.; Fang, T.; Konar, A.; Birdwell, A. G.; Nguyen, N. V.; Kis, A.; Jena, D.; Xing, H. G. *arXiv:1211.4136v1 [cond-mat.mtrl-sci]* **2012**,

(16) Benameur, M. M.; Radisavljevic, B.; Héron, J. S.; Sahoo, S.; Berger, H.; Kis, A. *Nanotechnology* **2011**, *22*, 125706.

(17) Kolosov, O.; Yamanaka, K. *Jpn. J. Appl. Phys.* **1993**, *7*.

(18) Yamanaka, K.; Ogiso, H.; Kolosov, O. *Appl. Phys. Lett.* **1994**, *64*, 178.

(19) McGuigan, A. P.; Huey, B. D.; Briggs, G. a. D.; Kolosov, O. V.; Tsukahara, Y.; Yanaka, M. *Appl. Phys. Lett.* **2002**, *80*, 1180.

(20) Mak, K. F.; He, K.; Lee, C.; Lee, G. H.; Hone, J.; Heinz, T. F. *Nature Materials* **2012**, *11*, 1–5.

(21) Dolui, K.; Rungger, I.; Sanvito, S. *Phys. Rev. B* **2013**, *87*, 165402.

(22) Zhan, Y.; Liu, Z.; Najmaei, S.; Ajayan, P. M.; Lou, J. *Small* **2012**, *8*, 966–971.

(23) Wolf, S. D.; Agostinelli, G.; Beaucarne, G.; Vitanov, P. *J. of Appl. Phys.* **2005**, *97*, 063303.

(24) Boogaard, A.; Kovalgin, A.; Wolters, R. *Microelectronic Engineering* **2009**, *86*, 1707–1710, Oxide charge; PECVD silicon oxide; Plasma oxidation.

(25) Zou, X.; Zhang, J. *Science China Technological Sciences* **2011**, *54*, 2123–2129.

(26) Peelaers, H.; Van de Walle, C. G. *Phys. Rev. B* **2012**, *86*, 241401.

(27) Zhang, X.; Han, W. P.; Wu, J. B.; Milana, S.; Lu, Y.; Li, Q. Q.; Ferrari, A. C.; Tan, P. H. *Phys. Rev. B* **2013**, *87*, 115413.